EUROPEAN ORGANIZATION FOR NUCLEAR RESEARCH

CERN–EP/99–81

10 June 1999

Measurement of the rate of $b\bar{b}b\bar{b}$ events in hadronic Z decays and the extraction of the gluon splitting into $b\bar{b}$

DELPHI Collaboration

Abstract

The rate $Z \to b\bar{b}b\bar{b}$ was measured using about 2×10^6 hadronic decays collected by the DELPHI experiment in 1994 and 1995. Events were forced into 3-jets with $y_{min} > 0.06$ and a b-tag was required for every jet. The rate was measured to be:

$$R_{4b} = \frac{BR(Z \to b\bar{b}b\bar{b})}{BR(Z \to hadrons)} = (6.0 \pm 1.9(stat.) \pm 1.4(syst.)) \times 10^{-4}$$

where the invariant mass of every $b\bar{b}$ system is above twice the b quark mass. Using the value of R_{4b} the probability of secondary production of a $b\bar{b}$ pair from a gluon per hadronic Z decay, $g_{b\bar{b}}$, was extracted and found to be:

$$g_{b\bar{b}} = (3.3 \pm 1.0(stat.) \pm 0.8(syst.)) \times 10^{-3}.$$

(Submitted to Physics Letters B)

P.Abreu[21], W.Adam[50], T.Adye[36], P.Adzic[11], I.Ajinenko[42], Z.Albrecht[17], T.Alderweireld[2], G.D.Alekseev[16], R.Alemany[49], T.Allmendinger[17], P.P.Allport[22], S.Almehed[24], U.Amaldi[9], N.Amapane[45], S.Amato[47], E.G.Anassontzis[3], P.Andersson[44], A.Andreazza[9], S.Andringa[21], P.Antilogus[25], W-D.Apel[17], Y.Arnoud[9], B.Åsman[44], J-E.Augustin[25], A.Augustinus[9], P.Baillon[9], A.Ballestrero[45], P.Bambade[19], F.Barao[21], G.Barbiellini[46], R.Barbier[25], D.Y.Bardin[16], G.Barker[17], A.Baroncelli[38], M.Battaglia[15], M.Baubillier[23], K-H.Becks[52], M.Begalli[6], A.Behrmann[52], P.Beilliere[8], Yu.Belokopytov[9,53], N.C.Benekos[31], A.C.Benvenuti[5], C.Berat[14], M.Berggren[25], D.Bertini[25], D.Bertrand[2], M.Besancon[39], M.Bigi[45], M.S.Bilenky[16], M-A.Bizouard[19], D.Bloch[10], H.M.Blom[30], M.Bonesini[27], W.Bonivento[27], M.Boonekamp[39], P.S.L.Booth[22], A.W.Borgland[4], G.Borisov[19], C.Bosio[41], O.Botner[48], E.Boudinov[30], B.Bouquet[19], C.Bourdarios[19], T.J.V.Bowcock[22], I.Boyko[16], I.Bozovic[11], M.Bozzo[13], P.Branchini[38], T.Brenke[52], R.A.Brenner[48], P.Bruckman[18], J-M.Brunet[8], L.Bugge[32], T.Buran[32], T.Burgsmueller[52], B.Buschbeck[50], P.Buschmann[52], S.Cabrera[49], M.Caccia[27], M.Calvi[27], T.Camporesi[9], V.Canale[37], F.Carena[9], L.Carroll[22], C.Caso[13], M.V.Castillo Gimenez[49], A.Cattai[9], F.R.Cavallo[5], V.Chabaud[9], Ph.Charpentier[9], L.Chaussard[25], P.Checchia[35], G.A.Chelkov[16], R.Chierici[45], P.Chliapnikov[42], P.Chochula[7], V.Chorowicz[25], J.Chudoba[29], K.Cieslik[18], P.Collins[9], R.Contri[13], E.Cortina[49], G.Cosme[19], F.Cossutti[9], J-H.Cowell[22], H.B.Crawley[1], D.Crennell[36], S.Crepe[14], G.Crosetti[13], J.Cuevas Maestro[33], S.Czellar[15], M.Davenport[9], W.Da Silva[23], A.Deghorain[2], G.Della Ricca[46], P.Delpierre[26], N.Demaria[9], A.De Angelis[9], W.De Boer[17], C.De Clercq[2], B.De Lotto[46], A.De Min[35], L.De Paula[47], H.Dijkstra[9], L.Di Ciaccio[37,9], J.Dolbeau[8], K.Doroba[51], M.Dracos[10], J.Drees[52], M.Dris[31], A.Duperrin[25], J-D.Durand[9], G.Eigen[4], T.Ekelof[48], G.Ekspong[44], M.Ellert[48], M.Elsing[9], J-P.Engel[10], B.Erzen[43], M.Espirito Santo[21], G.Fanourakis[11], D.Fassouliotis[11], J.Fayot[23], M.Feindt[17], P.Ferrari[27], A.Ferrer[49], E.Ferrer-Ribas[19], F.Ferro[13], S.Fichet[23], A.Firestone[1], U.Flagmeyer[52], H.Foeth[9], E.Fokitis[31], F.Fontanelli[13], B.Franek[36], A.G.Frodesen[4], R.Fruhwirth[50], F.Fulda-Quenzer[19], J.Fuster[49], A.Galloni[22], D.Gamba[45], S.Gamblin[19], M.Gandelman[47], C.Garcia[49], C.Gaspar[9], M.Gaspar[47], U.Gasparini[35], Ph.Gavillet[9], E.N.Gazis[31], D.Gele[10], L.Gerdyukov[42], N.Ghodbane[25], I.Gil[49], F.Glege[52], R.Gokieli[9,51], B.Golob[43], G.Gomez-Ceballos[40], P.Goncalves[21], I.Gonzalez Caballero[40], G.Gopal[36], L.Gorn[1,54], Yu.Gouz[42], V.Gracco[13], J.Grahl[1], E.Graziani[38], C.Green[22], H-J.Grimm[17], P.Gris[39], G.Grosdidier[19], K.Grzelak[51], M.Gunther[48], J.Guy[36], F.Hahn[9], S.Hahn[52], S.Haider[9], A.Hallgren[48], K.Hamacher[52], J.Hansen[32], F.J.Harris[34], V.Hedberg[24], S.Heising[17], J.J.Hernandez[49], P.Herquet[2], H.Herr[9], T.L.Hessing[34], J.-M.Heuser[52], E.Higon[49], S-O.Holmgren[44], P.J.Holt[34], S.Hoorelbeke[2], M.Houlden[22], J.Hrubec[50], K.Huet[2], G.J.Hughes[22], K.Hultqvist[44], J.N.Jackson[22], R.Jacobsson[9], P.Jalocha[9], R.Janik[7], Ch.Jarlskog[24], G.Jarlskog[24], P.Jarry[39], B.Jean-Marie[19], E.K.Johansson[44], P.Jonsson[25], C.Joram[9], P.Juillot[10], F.Kapusta[23], K.Karafasoulis[11], S.Katsanevas[25], E.C.Katsoufis[31], R.Keranen[17], B.P.Kersevan[43], B.A.Khomenko[16], N.N.Khovanski[16], A.Kiiskinen[15], B.King[22], A.Kinvig[22], N.J.Kjaer[30], O.Klapp[52], H.Klein[9], P.Kluit[30], P.Kokkinias[11], M.Koratzinos[9], V.Kostioukhine[42], C.Kourkoumelis[3], O.Kouznetsov[39], M.Krammer[50], E.Kriznic[43], J.Krstic[11], Z.Krumstein[16], P.Kubinec[7], J.Kurowska[51], K.Kurvinen[15], J.W.Lamsa[1], D.W.Lane[1], P.Langefeld[52], V.Lapin[42], J-P.Laugier[39], R.Lauhakangas[15], G.Leder[50], F.Ledroit[14], V.Lefebure[2], L.Leinonen[44], A.Leisos[11], R.Leitner[29], J.Lemonne[2], G.Lenzen[52], V.Lepeltier[19], T.Lesiak[18], M.Lethuillier[39], J.Libby[34], D.Liko[9], A.Lipniacka[44], I.Lippi[35], B.Loerstad[24], J.G.Loken[34], J.H.Lopes[47], J.M.Lopez[40], R.Lopez-Fernandez[14], D.Loukas[11], P.Lutz[39], L.Lyons[34], J.MacNaughton[50], J.R.Mahon[6], A.Maio[21], A.Malek[52], T.G.M.Malmgren[44], S.Maltezos[31], V.Malychev[16], F.Mandl[50], J.Marco[40], R.Marco[40], B.Marechal[47], M.Margoni[35], J-C.Marin[9], C.Mariotti[9], A.Markou[11], C.Martinez-Rivero[19], F.Martinez-Vidal[49], S.Marti i Garcia[9], J.Masik[12], N.Mastroyiannopoulos[11], F.Matorras[40], C.Matteuzzi[27], G.Matthiae[37], F.Mazzucato[35], M.Mazzucato[35], M.Mc Cubbin[22], R.Mc Kay[1], R.Mc Nulty[22], G.Mc Pherson[22], C.Meroni[27], W.T.Meyer[1], A.Miagkov[42], E.Migliore[45], L.Mirabito[25], W.A.Mitaroff[50], U.Mjoernmark[24], T.Moa[44], M.Moch[17], R.Moeller[28], K.Moenig[9], M.R.Monge[13], X.Moreau[23], P.Morettini[13], G.Morton[34], U.Mueller[52], K.Muenich[52], M.Mulders[30], C.Mulet-Marquis[14], R.Muresan[24], W.J.Murray[36], B.Muryn[14,18], G.Myatt[34], T.Myklebust[32], F.Naraghi[14], M.Nassiakou[11], F.L.Navarria[5], S.Navas[49], K.Nawrocki[51], P.Negri[27], S.Nemecek[12], N.Neufeld[9], R.Nicolaidou[39], B.S.Nielsen[28], P.Niezurawski[51], M.Nikolenko[10,16], V.Nomokonov[15], A.Normand[22], A.Nygren[24], V.Obraztsov[42], A.G.Olshevski[16], A.Onofre[21], R.Orava[15], G.Orazi[10], K.Osterberg[15], A.Ouraou[39], M.Paganoni[27], S.Paiano[5], R.Pain[23], R.Paiva[21], J.Palacios[34], H.Palka[18], Th.D.Papadopoulou[31,9], K.Papageorgiou[11], L.Pape[9], C.Parkes[9], F.Parodi[13], U.Parzefall[22], A.Passeri[38], O.Passon[52], M.Pegoraro[35], L.Peralta[21], M.Pernicka[50], A.Perrotta[5], C.Petridou[46], A.Petrolini[13], H.T.Phillips[36], F.Pierre[39], M.Pimenta[21], E.Piotto[27], T.Podobnik[43], M.E.Pol[6], G.Polok[18], P.Poropat[46], V.Pozdniakov[16], P.Privitera[37], N.Pukhaeva[16], A.Pullia[27], D.Radojicic[34], S.Ragazzi[27], H.Rahmani[31], P.N.Ratoff[20], A.L.Read[32], P.Rebecchi[9], N.G.Redaelli[27], M.Regler[50], D.Reid[30], R.Reinhardt[52], P.B.Renton[34], L.K.Resvanis[3], F.Richard[19], J.Ridky[12], G.Rinaudo[45], O.Rohne[32], A.Romero[45], P.Ronchese[35], E.I.Rosenberg[1], P.Rosinsky[7], P.Roudeau[19], T.Rovelli[5], Ch.Royon[39], V.Ruhlmann-Kleider[39], A.Ruiz[40], H.Saarikko[15], Y.Sacquin[39], A.Sadovsky[16], G.Sajot[14], J.Salt[49], D.Sampsonidis[11], M.Sannino[13], H.Schneider[17], Ph.Schwemling[23], B.Schwering[52], U.Schwickerath[17], M.A.E.Schyns[52], F.Scuri[46], P.Seager[20], Y.Sedykh[16], A.M.Segar[34], R.Sekulin[36], R.C.Shellard[6], A.Sheridan[22], M.Siebel[52], L.Simard[39], F.Simonetto[35], A.N.Sisakian[16], G.Smadja[25], N.Smirnov[42], O.Smirnova[24], G.R.Smith[36], A.Sopczak[17], R.Sosnowski[51], T.Spassov[21], E.Spiriti[38], P.Sponholz[52], S.Squarcia[13], C.Stanescu[38], S.Stanic[43], K.Stevenson[34], A.Stocchi[19], R.Strub[10], B.Stugu[4], M.Szczekowski[51], M.Szeptycka[51], T.Tabarelli[27], O.Tchikilev[42], F.Tegenfeldt[48], F.Terranova[27], J.Thomas[34], J.Timmermans[30], N.Tinti[5], L.G.Tkatchev[16], S.Todorova[10], A.Tomaradze[2], B.Tome[21], A.Tonazzo[9], L.Tortora[38], G.Transtromer[24], D.Treille[9], G.Tristram[8],

M.Trochimczuk[51], C.Troncon[27], A.Tsirou[9], M-L.Turluer[39], I.A.Tyapkin[16], S.Tzamarias[11], O.Ullaland[9], V.Uvarov[42], G.Valenti[5], E.Vallazza[46], C.Vander Velde[2], G.W.Van Apeldoorn[30], P.Van Dam[30], W.K.Van Doninck[2], J.Van Eldik[30], A.Van Lysebetten[2], N.Van Remortel[2], I.Van Vulpen[30], N.Vassilopoulos[34], G.Vegni[27], L.Ventura[35], W.Venus[36,9], F.Verbeure[2], M.Verlato[35], L.S.Vertogradov[16], V.Verzi[37], D.Vilanova[39], L.Vitale[46], E.Vlasov[42], A.S.Vodopyanov[16], C.Vollmer[17], G.Voulgaris[3], V.Vrba[12], H.Wahlen[52], C.Walck[44], C.Weiser[17], D.Wicke[52], J.H.Wickens[2], G.R.Wilkinson[9], M.Winter[10], M.Witek[18], G.Wolf[9], J.Yi[1], O.Yushchenko[42], A.Zalewska[18], P.Zalewski[51], D.Zavrtanik[43], E.Zevgolatakos[11], N.I.Zimin[16,24], G.C.Zucchelli[44], G.Zumerle[35]

[1] Department of Physics and Astronomy, Iowa State University, Ames IA 50011-3160, USA
[2] Physics Department, Univ. Instelling Antwerpen, Universiteitsplein 1, BE-2610 Wilrijk, Belgium
and IIHE, ULB-VUB, Pleinlaan 2, BE-1050 Brussels, Belgium
and Faculté des Sciences, Univ. de l'Etat Mons, Av. Maistriau 19, BE-7000 Mons, Belgium
[3] Physics Laboratory, University of Athens, Solonos Str. 104, GR-10680 Athens, Greece
[4] Department of Physics, University of Bergen, Allégaten 55, NO-5007 Bergen, Norway
[5] Dipartimento di Fisica, Università di Bologna and INFN, Via Irnerio 46, IT-40126 Bologna, Italy
[6] Centro Brasileiro de Pesquisas Físicas, rua Xavier Sigaud 150, BR-22290 Rio de Janeiro, Brazil
and Depto. de Física, Pont. Univ. Católica, C.P. 38071 BR-22453 Rio de Janeiro, Brazil
and Inst. de Física, Univ. Estadual do Rio de Janeiro, rua São Francisco Xavier 524, Rio de Janeiro, Brazil
[7] Comenius University, Faculty of Mathematics and Physics, Mlynska Dolina, SK-84215 Bratislava, Slovakia
[8] Collège de France, Lab. de Physique Corpusculaire, IN2P3-CNRS, FR-75231 Paris Cedex 05, France
[9] CERN, CH-1211 Geneva 23, Switzerland
[10] Institut de Recherches Subatomiques, IN2P3 - CNRS/ULP - BP20, FR-67037 Strasbourg Cedex, France
[11] Institute of Nuclear Physics, N.C.S.R. Demokritos, P.O. Box 60228, GR-15310 Athens, Greece
[12] FZU, Inst. of Phys. of the C.A.S. High Energy Physics Division, Na Slovance 2, CZ-180 40, Praha 8, Czech Republic
[13] Dipartimento di Fisica, Università di Genova and INFN, Via Dodecaneso 33, IT-16146 Genova, Italy
[14] Institut des Sciences Nucléaires, IN2P3-CNRS, Université de Grenoble 1, FR-38026 Grenoble Cedex, France
[15] Helsinki Institute of Physics, HIP, P.O. Box 9, FI-00014 Helsinki, Finland
[16] Joint Institute for Nuclear Research, Dubna, Head Post Office, P.O. Box 79, RU-101 000 Moscow, Russian Federation
[17] Institut für Experimentelle Kernphysik, Universität Karlsruhe, Postfach 6980, DE-76128 Karlsruhe, Germany
[18] Institute of Nuclear Physics and University of Mining and Metalurgy, Ul. Kawiory 26a, PL-30055 Krakow, Poland
[19] Université de Paris-Sud, Lab. de l'Accélérateur Linéaire, IN2P3-CNRS, Bât. 200, FR-91405 Orsay Cedex, France
[20] School of Physics and Chemistry, University of Lancaster, Lancaster LA1 4YB, UK
[21] LIP, IST, FCUL - Av. Elias Garcia, 14-1^{o}, PT-1000 Lisboa Codex, Portugal
[22] Department of Physics, University of Liverpool, P.O. Box 147, Liverpool L69 3BX, UK
[23] LPNHE, IN2P3-CNRS, Univ. Paris VI et VII, Tour 33 (RdC), 4 place Jussieu, FR-75252 Paris Cedex 05, France
[24] Department of Physics, University of Lund, Sölvegatan 14, SE-223 63 Lund, Sweden
[25] Université Claude Bernard de Lyon, IPNL, IN2P3-CNRS, FR-69622 Villeurbanne Cedex, France
[26] Univ. d'Aix - Marseille II - CPP, IN2P3-CNRS, FR-13288 Marseille Cedex 09, France
[27] Dipartimento di Fisica, Università di Milano and INFN, Via Celoria 16, IT-20133 Milan, Italy
[28] Niels Bohr Institute, Blegdamsvej 17, DK-2100 Copenhagen Ø, Denmark
[29] NC, Nuclear Centre of MFF, Charles University, Areal MFF, V Holesovickach 2, CZ-180 00, Praha 8, Czech Republic
[30] NIKHEF, Postbus 41882, NL-1009 DB Amsterdam, The Netherlands
[31] National Technical University, Physics Department, Zografou Campus, GR-15773 Athens, Greece
[32] Physics Department, University of Oslo, Blindern, NO-1000 Oslo 3, Norway
[33] Dpto. Fisica, Univ. Oviedo, Avda. Calvo Sotelo s/n, ES-33007 Oviedo, Spain
[34] Department of Physics, University of Oxford, Keble Road, Oxford OX1 3RH, UK
[35] Dipartimento di Fisica, Università di Padova and INFN, Via Marzolo 8, IT-35131 Padua, Italy
[36] Rutherford Appleton Laboratory, Chilton, Didcot OX11 OQX, UK
[37] Dipartimento di Fisica, Università di Roma II and INFN, Tor Vergata, IT-00173 Rome, Italy
[38] Dipartimento di Fisica, Università di Roma III and INFN, Via della Vasca Navale 84, IT-00146 Rome, Italy
[39] DAPNIA/Service de Physique des Particules, CEA-Saclay, FR-91191 Gif-sur-Yvette Cedex, France
[40] Instituto de Fisica de Cantabria (CSIC-UC), Avda. los Castros s/n, ES-39006 Santander, Spain
[41] Dipartimento di Fisica, Università degli Studi di Roma La Sapienza, Piazzale Aldo Moro 2, IT-00185 Rome, Italy
[42] Inst. for High Energy Physics, Serpukov P.O. Box 35, Protvino, (Moscow Region), Russian Federation
[43] J. Stefan Institute, Jamova 39, SI-1000 Ljubljana, Slovenia and Laboratory for Astroparticle Physics,
Nova Gorica Polytechnic, Kostanjeviska 16a, SI-5000 Nova Gorica, Slovenia,
and Department of Physics, University of Ljubljana, SI-1000 Ljubljana, Slovenia
[44] Fysikum, Stockholm University, Box 6730, SE-113 85 Stockholm, Sweden
[45] Dipartimento di Fisica Sperimentale, Università di Torino and INFN, Via P. Giuria 1, IT-10125 Turin, Italy
[46] Dipartimento di Fisica, Università di Trieste and INFN, Via A. Valerio 2, IT-34127 Trieste, Italy
and Istituto di Fisica, Università di Udine, IT-33100 Udine, Italy
[47] Univ. Federal do Rio de Janeiro, C.P. 68528 Cidade Univ., Ilha do Fundão BR-21945-970 Rio de Janeiro, Brazil
[48] Department of Radiation Sciences, University of Uppsala, P.O. Box 535, SE-751 21 Uppsala, Sweden
[49] IFIC, Valencia-CSIC, and D.F.A.M.N., U. de Valencia, Avda. Dr. Moliner 50, ES-46100 Burjassot (Valencia), Spain
[50] Institut für Hochenergiephysik, Österr. Akad. d. Wissensch., Nikolsdorfergasse 18, AT-1050 Vienna, Austria
[51] Inst. Nuclear Studies and University of Warsaw, Ul. Hoza 69, PL-00681 Warsaw, Poland
[52] Fachbereich Physik, University of Wuppertal, Postfach 100 127, DE-42097 Wuppertal, Germany
[53] On leave of absence from IHEP Serpukhov
[54] Now at University of Florida

1 Introduction

The production of b quarks in e^+e^- annihilation at the Z mass receives contributions from two sources, namely the annihilation itself and the splitting of gluons emitted from quarks, $e^+e^- \to q\bar{q}g, g \to b\bar{b}$. The latter is usually called *secondary* b production. While the ratio $R_b = \sigma(e^+e^- \to b\bar{b})/\sigma(e^+e^- \to \text{ hadrons})$ has been measured with very high precision [1,2], the secondary production of b quarks is comparatively poorly known [3]. Though being interesting in its own, it is usually considered as a source of background for the study of $e^+e^- \to b\bar{b}$ processes and is, in fact, one of the main sources of uncertainty on the measurement of R_b [1,2].

In this analysis the rate of events showing both primary and secondary production of b quarks, $R_{4b} = \frac{BR(Z \to b\bar{b}b\bar{b})}{BR(Z \to \text{hadrons})}$, is measured for the first time at LEP. From this measurement g_{bb}, the rate of events with secondary b-quark production per hadronic Z decay, is estimated. Interference and mass effects between the four massive b-quarks, absent at leading order for $q\bar{q}b\bar{b}$ events (q massless) [4], are taken into account using theoretical computations.

In 1994 and 1995 a sample of 2 million Z decays was collected at LEP by the DELPHI experiment with a new Vertex Detector [5] capable of measuring the coordinates of points on tracks in three dimensions, thus considerably improving the b-tagging performance. The improved b-tagging efficiency allows the measurement of R_{4b} with the identification of at least three jets produced by the hadronization of a b quark. Since events are forced into a 3-jet topology no sharp drop in signal efficiency as a function of the minimum invariant mass of the $b\bar{b}$ pair was found down to twice the b quark mass, $2 \times m_b$.

2 The DELPHI Detector

The DELPHI detector and its performance have been described in detail in ref. [6]. Here only the Vertex Detector (VD) [5], the most relevant detector used in this analysis, will be described.

The VD is the innermost detector in DELPHI. It is located between the LEP beam pipe and the Inner Detector. In 1994 the original DELPHI Vertex Detector [7] was upgraded to provide a three-dimensional readout [5]. It consists of three concentric layers of silicon microstrip detectors at radii of 6.3, 9 and 11 cm from the beam line, called the closer, inner and outer layer respectively. The microstrip detectors of the closer and outer layers provide hits in the $R\Phi$ and the Rz-plane [1], while for the inner layer only the $R\Phi$ coordinate is measured. For polar angles of $44° \leq \theta \leq 136°$ a track crosses all the three silicon layers of the VD. The closer layer covers the polar region between 25° and 155°. The measured intrinsic precision is about 8 μm for the $R\Phi$ measurement while for z it depends on the polar angle of the incident track, and goes from about 10 μm for tracks perpendicular to the modules to 20 μm for tracks with a polar angle of 25°. For charged particle tracks with hits in all three $R\Phi$ VD layers, the impact parameter[2] precision is $\sigma_{R\Phi} = [61/(p\sin^{3/2}\theta) \oplus 20]\mu$m while for tracks with hits in both the Rz layers it is $\sigma_z = [67/(p\sin^{5/2}\theta) \oplus 33]\mu$m, where p is the momentum in GeV/c.

[1] In the DELPHI coordinate system z is along the beam line, Φ is the azimuthal angle in the xy plane, R is the radius and θ is the polar angle with respect to the z axis.

[2] The impact parameter is defined as the distance of closest approach of a charged particle to the reconstructed primary vertex.

3 Analysis and Results

3.1 The Identification of b Jets

The b-tagging method used in this analysis is described in detail in ref.[1]. It acts on clusters of particles (jets), obtained in this analysis with the DURHAM [8] algorithm, combining four different variables defined for each jet. The first variable P_J^+, originally proposed by ALEPH [9] and further developed by DELPHI [1,10], represents the probability that, in a given jet, all the tracks with positive impact parameter originate from the primary vertex. The track impact parameters are computed separately in the $R\Phi$ plane and along the z direction. The sign of the impact parameter is defined with respect to the jet direction. It is positive if the point of closest approach of the track to the jet axis is downstream of the primary vertex along the jet direction, and negative if it is upstream. In this way the same sign is assigned to the $R\Phi$ and z impact parameters. Additional selection variables are defined only for the jets where a secondary vertex is reconstructed. They are: the effective mass, the rapidity with respect to the jet direction and the energy of the charged particles included in the secondary vertex. Reconstructed secondary vertices are accepted if $L/\sigma_L \geq 4$ where L is the distance from the primary vertex and σ_L is its uncertainty, which happens in about 55% of the jets with b-quarks. Whenever a secondary vertex is reconstructed, the jet direction is recomputed as the direction from the primary vertex to the secondary vertex and the sign of the impact parameter is redefined accordingly.

For a given selection variable, x, the ratio of the probability density function for background $f^B(x)$ and for signal events $f^S(x)$ is defined to be $y = f^B(x)/f^S(x)$. In the case of several independent variables the corresponding definition is:

$$y = \frac{f^B(x_1, \ldots, x_n)}{f^S(x_1, \ldots, x_n)} = \prod \frac{f_i^B(x_i)}{f_i^S(x_i)} = \prod y_i \,. \tag{1}$$

The jet is tagged as containing a b quark if the discriminating variable $\eta = -\log_{10} y > \eta_0$; the choice of η_0 defines the efficiency and purity of the sample.

3.2 Event Selection

The criteria to identify hadronic Z decays are the following. Charged particles were accepted if:

- their track length was larger than 30 cm;
- their impact parameter was less than 4 cm in the $R\Phi$ plane and less than 10 cm in z;
- their momentum was larger than 400 MeV/c;
- the relative error σ_p/p was less than 1, where p is the momentum.

Since the VD dominates the impact parameter resolution, only tracks with VD information were used for the b-tagging. In particular, both for the probability computation and the secondary vertex reconstruction, the $R\Phi$ information of the tracks was used only if they had at least one $R\Phi$ VD hit while for the Rz information at least one Rz hit and two $R\Phi$ hits in the VD were required. Neutral particles were accepted if their energy deposition was larger than 700 MeV in the barrel electromagnetic calorimeter or 400 MeV in the forward calorimeter. Neutral particles were used in the reconstruction of the jet direction; their selection was therefore optimised for this purpose.

Hadronic Z decays were selected by requiring:

- at least six charged particles;
- the summed energy of the charged particles to be larger than 12% of the centre-of-mass energy.

Only events collected while the Vertex Detector and the Time Projection Chamber were fully operational were accepted. With these requirements, about 1,400,000 and 600,000 Z events were selected in the 1994 and 1995 data samples respectively, with an efficiency above 97%. The contamination due to $\tau^+\tau^-$ and $\gamma\gamma$ events was estimated to be below 0.6%. The corresponding contribution was subtracted from the measured data.

Simulated events were generated using the JETSET 7.3 parton shower (PS) Monte Carlo program [11] tuned for the DELPHI data. The response of the DELPHI detector was simulated in full detail using the DELSIM program [6]. A good simulation of the impact parameter and the b-tagging variables for Z decays into light quarks (u,d,s,c) is very important in this analysis; for this reason a fine tuning of the $R\Phi$ and z impact parameter resolutions has been developed and applied [10]. Three samples consisting of 5.0×10^6 hadronic Z decays, 3.0×10^6 $Z \rightarrow b\bar{b}$ events and 2×10^4 $Z \rightarrow b\bar{b}b\bar{b}$ events were used[3]. An additional sample of 10^4 $b\bar{b}b\bar{b}$ events was produced with the JETSET Matrix Element Monte Carlo generator [12] and used to test the model dependence of the result.

Simulated events were reweighted according to the latest LEP Heavy Flavour Working Group recommendations [13]. In particular, the rate of gluon splitting to c quarks, $g_{c\bar{c}}$, was set to 2.33%.

3.3 Selection of $b\bar{b}b\bar{b}$ Events and Results

The selection is based on the identification of 3 b-originated jets in the event.
Events can be grouped in four categories:

- Signal events (***4B*** events);
- Events with primary b production and gluon splitting to $c\bar{c}$ (***C*** events);
- Events with primary b production but no gluon splitting to heavy quarks (***2B*** events);
- All other events, i.e. without primary b production (***Q*** events).

The efficiencies of selecting these classes of events after all cuts are indicated with $\epsilon_{4b}, \epsilon_c, \epsilon_{2b}, \epsilon_q$ respectively.

First, events in the very forward region were discarded by means of a cut on the thrust direction, $|\cos\theta_T| < 0.9$.

Reconstructed tracks were clustered into 3 jets in each event using the DURHAM algorithm. Genuine two-jet-like events were rejected with a cut on the variable y_{min}[4]. Fixing the number of jets to three has the result, for events with higher jet multiplicity, of joining the nearest jets, which in most cases are those produced by the gluon splitting process. This increases the efficiency of the b-tagging selection which grows with the number of tracks used [1].

Figure 1 shows the distributions of y_{min} for data and simulated events. Events with $y_{min} < 0.06$ were rejected, thus removing as many as possible of the events which contained no gluon splitting, while retaining a good fraction of the signal. According to the simulation, the efficiency of the selection for signal events after the cut on the variable

[3] Since the detector did not change between 1994 and 1995 and the efficiencies of selecting signal and background events obtained with the description of the detector for those years are compatible within their error, events simulated for 1994 and 1995 are considered together here and in the following.

[4] The variable y_{min} is defined as the DURHAM distance between the two nearest jets in the event.

y_{min} was $(46.3 \pm 0.3)\%$. The discrepancy between data and simulation in the fraction of selected events was found to be

$$\frac{f_{3-jet}^{DATA}}{f_{3-jet}^{SIM}} = 0.961 \pm 0.003\,. \tag{2}$$

After this selection, jets were sorted using the b-tagging variable η (cf. Eq. 1), jet 1 being the one with the highest probability to contain tracks from b decay. This allows a separate choice of the three cut values. Figure 2 shows the distributions of η for the three ordered jets for data and simulation.
The values for the three η cuts were chosen in order to minimise the final relative error on R_{4b} and were 0.9, 0.2, and -0.1 for the three ordered jets respectively. With this requirement, 140 events were selected in the data sample.

The data-Monte Carlo discrepancy of Eq. 2 was taken into account attributing it to ***2B*** and ***Q*** background events (99.4% of the initial Monte Carlo sample). The efficiency ϵ_{2b} was rescaled from $(0.0161 \pm 0.0006)\%$ to $(0.0154 \pm 0.0006)\%$. In the ***Q*** category only one event was selected by the cuts with an efficiency compatible with zero $(0.000025 \pm 0.000025)\%$.

For the efficiencies of tagging b-jets which correspond to our cuts, the analysis of R_b [1] found a 3% discrepancy between data and simulation. This discrepancy can be explained by the uncertainties in the description of b-hadrons production and decay and it was found to be stable within 1% as a function of the jet momentum. The background efficiencies ϵ_c and ϵ_{2b} were therefore corrected by a factor 1.06 ± 0.02 and the signal efficiency ϵ_{4b} by a factor 1.09 ± 0.05. In case of signal events the uncertainty follows from the conservative assumption that, for the jet containing the two b-hadrons, the error on the rescaling factor is equal to the full size of the correction itself. The uncertainties on these coefficients were used to estimate a systematic error (cf. sec. 3.4). The efficiencies of the different classes of events are summarised in Table 1.

Event type	Efficiency (%)	Purity (%)
4B	$\epsilon_{4b} = 3.16 \pm 0.11$	$f_{4b} \sim 24$
C	$\epsilon_c = 0.321 \pm 0.023$	$f_c \sim 23$
2B	$\epsilon_{2b} = 0.0164 \pm 0.0006$	$f_{2b} \sim 53$
Q	$\epsilon_q = 0.00002 \pm 0.00002$	$f_q \sim 0$

Table 1: *Total efficiencies and sample composition for the different classes of events in the simulation. The values in the table account for the corrections discussed in sec. 3.3. The sample composition is approximate as it depends on the assumed value of* R_{4b}.

The rate of $b\bar{b}b\bar{b}$ events can then be extracted from the relation

$$R_{4b} = \frac{f_d - \epsilon_q - R_b[g_{cc}(\epsilon_c - \epsilon_{2b}) + \epsilon_{2b} - \epsilon_q]}{\epsilon_{4b} - \epsilon_{2b}} \tag{3}$$

where f_d is the fraction of events selected in data, R_b is set to the world average value [14] of 0.21656 ± 0.00074 and $g_{cc} = (2.33 \pm 0.50)\%$ is the value of the gluon splitting probability to c quarks measured by OPAL [15]. The term ϵ_{2b} appears in the denominator since ***4B*** events are a subsample of $Z \to b\bar{b}$ events.

The measured value is

$$R_{4b} = (6.0 \pm 1.9(stat.)) \times 10^{-4}\,. \tag{4}$$

Figure 3 shows the stability of the result as a function of the cut on y_{min} and figure 4 as a function of the cuts on the b-tagging variables of the three ordered jets. The distribution of the b-tagging variable for the third jet after all the other cuts for data and simulation is shown in figure 5.

3.4 Systematic Uncertainties

The following contributions were considered:

Data-Monte Carlo discrepancy in the y_{min} cut. The rescaling of ϵ_{2b} and ϵ_q to account for the discrepancy of Eq. 2 was made under the assumption that the gluon splitting process to b and c quarks is correctly described by the JETSET PS Monte Carlo generator. A systematic uncertainty was therefore estimated assigning the discrepancy to both signal and background. This gave a contribution of $\pm 0.25 \times 10^{-4}$ to the systematic error.

B-tagging. As described in sec. 3.3, the signal efficiency ϵ_{4b} was rescaled by 1.09 ± 0.05 and the background efficiencies ϵ_c and ϵ_{2b} by 1.06 ± 0.02. A systematic uncertainty on the b-tagging efficiency was estimated varying these factors by their error. This gave a contribution of $\pm 0.36 \times 10^{-4}$ to the final error.

Charm quark mistagging probability. The limited knowledge of charm decays affects the value of the efficiency ϵ_c. A systematic uncertainty was estimated varying the efficiency for tagging a jet containing a D meson by $\pm 10\%$. The corresponding contribution to the systematic error is $\pm 0.45 \times 10^{-4}$.

γ, K^0 and Λ production rates. Jets with non-reconstructed γ, K^0 and Λ can be wrongly identified as b-jets. The production rates of these particles were varied in the simulation by $\pm 50\%$, $\pm 10\%$ and $\pm 15\%$ respectively, i.e. by the amount of the difference of reconstruction efficiency in data and simulation. This led to a contribution of $\pm 0.06 \times 10^{-4}$ to the systematic error.

Value of g_{cc} and R_b . Varying R_b and g_{cc} in Eq. 3 by their error results in contributions to the systematic error of $\pm 0.055 \times 10^{-4}$ and $\pm 1.05 \times 10^{-4}$ respectively.

Model Dependence. To test the dependence of the result on the model used to simulate signal events, the same selection was repeated on a dedicated sample of 10^4 signal events generated with JETSET Matrix Element [12]. The resulting efficiency is $\epsilon_{4b}^{ME} = (3.34 \pm 0.18)\%$. The statistical uncertainty on the difference between the two efficiencies was conservatively taken as the systematic error, resulting in $\Delta R_{4b} = \pm 0.40 \times 10^{-4}$.

The effect of a different fragmentation model on the three-jet rate in the simulation was tested using the HERWIG [16] event generator. The ratio of the three-jet rates of hadrons and partons at generator level was studied as a function of the y_{min} cut for HERWIG 5.9 and JETSET 7.4. The maximum discrepancy found between the two generators was $\pm 2\%$. The effect of this difference on the rescaling factor of Eq. 2 produces a change $\Delta R_{4b} = \pm 0.23 \times 10^{-4}$. Adding in quadrature the two contributions results in a total uncertainty due to the Monte Carlo model $\Delta R_{4b} = 0.46 \times 10^{-4}$.

Monte Carlo statistics. The limited Monte Carlo statistics gave a contribution of $\pm 0.61 \times 10^{-4}$ to the systematic error.

The total systematic error amounts to $\pm 1.4 \times 10^{-4}$. All systematic errors considered are summarised in table 2.

Source of systematics	Range	$\Delta R_{4b} \times 10^4$
Data/MC (y_{min})		∓ 0.25
b-tagging		∓ 0.36
Charm efficiency		∓ 0.45
γ, K^0, Λ	$\pm 50\%$, $\pm 10\%$, $\pm 15\%$	∓ 0.06
g_{cc}	$(2.33 \pm 0.50)\%$	∓ 1.05
R_b	$(21.656 \pm 0.074)\%$	∓ 0.055
MC model		± 0.46
MC statistics		± 0.61
Total		± 1.44

Table 2: *Systematic errors on the measurement of* R_{4b}

3.5 The Extraction of $g_{b\bar{b}}$

The gluon splitting probability $g_{b\bar{b}}$ is the fraction of hadronic Z decays with a gluon coupled to a $b\bar{b}$ pair:

$$g_{b\bar{b}} = \frac{\mathrm{BR}(Z \to q\bar{q}g, g \to b\bar{b})}{\mathrm{BR}(Z \to \mathrm{hadrons})}$$

where the numerator is calculated summing on all flavours (q=u,d,s,c,b). This relation can be re-expressed in term of the measured rate of $b\bar{b}b\bar{b}$ events:

$$g_{b\bar{b}} = R_{4b} \times \frac{\mathrm{BR}(Z \to q\bar{q}g, g \to b\bar{b})}{\mathrm{BR}(Z \to b\bar{b}b\bar{b})} = R_{4b} \times R_{th} \qquad (5)$$

The term R_{th} of Eq. 5 depends weakly on the theoretical parameters α_S and m_b since the dependence is suppressed in the ratio of the two branching ratios. For the extraction of $g_{b\bar{b}}$, R_{th} was computed using the WPHACT program [18] which properly accounts for the interference term between primary and secondary heavy quark production which are not separated in this analysis.

The theoretical estimation of the branching ratios depends on the minimum invariant mass between the pair of quarks over which the integration is performed. The cutoff values in the simulation are:

- 2.25 GeV/c^2 for light quarks. This value is set equal to the JETSET Q_0 parameter determined by the DELPHI JETSET tuning [17];
- twice the pole mass of the b quark, m_b, for the $b\bar{b}$ system. The value of m_b is set to 4.7 GeV/c^2 in the JETSET PS Monte Carlo generator.

Therefore R_{th} was evaluated with the following cuts on the invariant masses of quark pairs: 2.25 GeV/c^2, 5.82 GeV/c^2, 9.4 GeV/c^2 for $q\bar{q}$, qb and $b\bar{b}$ respectively. For $m_b = 4.7$ GeV/c^2 and α_S running we obtain $R_{th} = 5.457 \pm 0.008$ where the error takes into account the numerical accuracy of the calculation only. Inserting this value in Eq. 5 we get

$$g_{b\bar{b}} = (3.3 \pm 1.0(stat.) \pm 0.8(syst.)) \times 10^{-3}\,.$$

The effect of the value of m_b on the extraction of $g_{b\bar{b}}$ was investigated recomputing R_{th} for $m_b = 3$ GeV/c^2 and with the same set of cuts on the invariant masses of quark pairs. The value obtained is $R_{th} = 5.660 \pm 0.010$. From this we get $g_{b\bar{b}} = (3.4 \pm 1.1(stat.) \pm 0.8(syst.)) \times 10^{-3}$.

The signal efficiency as a function of the minimum invariant mass between $b\bar{b}$ pair is shown in figure 6. It can be seen that the analysis is fully sensitive down to the cutoff value set in the simulation.

The dependence of R_{th} on the cut on the minimum invariant mass of non $b\bar{b}$ pair was checked extending the integration down to 1 GeV/c^2 for $q\bar{q}$ pairs and to 5.2 GeV/c^2 for qb pairs. The corresponding relative changes in R_{th} were found to be less than 1%.

4 Conclusions

The rate of events with four b quarks in the final state was measured. Events were selected by clustering tracks into three jets and each one was required to pass the b-tagging selection. Two-jet like events were discarded using a cut on the y_{min} variable.

As result, we obtained

$$R_{4b} = (6.0 \pm 1.9(stat.) \pm 1.4(syst.)) \times 10^{-4}$$

where the first error is statistical and the second includes all systematic effects.

From R_{4b} we estimate the rate of secondary b quarks to be:

$$g_{bb} = (3.3 \pm 1.0(stat.) \pm 0.8(syst.)) \times 10^{-3}$$

This value is in agreement with previous measurements of DELPHI and ALEPH [3]. Both of them used a method different from the one described in this paper. They considered the process $Z \to q\bar{q}g, g \to b\bar{b}$ (q=u,d,s,c,b). Events were selected reconstructing four jets and applying the b-tagging on the two jets which were more likely to come from the gluon splitting process. Additional cuts were applied in order to suppress the background of $Z \to b\bar{b}g, g \to q\bar{q}$ (q=u,d,s,c). This approach was therefore based on the separation of primary and secondary b production, relying on the Monte Carlo model. Moreover in their analysis, the selection of four-jet events implicitly constrained the available phase space.

The approach used in the present analysis, based on the selection of four-b events, results in a smaller statistics, but the dependence on the Monte Carlo model is reduced, because there is no need to distinguish primary and secondary b quark production. In addition, the use of a three-jet topology opens the measurement to all the available phase space, in particular to the region of low values of invariant mass of the $b\bar{b}$ pairs.

Acknowledgements

We are greatly indebted to our technical collaborators, to the members of the CERN-SL Division for the excellent performance of the LEP collider, and to the funding agencies for their support in building and operating the DELPHI detector.
We acknowledge in particular the support of
Austrian Federal Ministry of Science and Traffics, GZ 616.364/2-III/2a/98,
FNRS–FWO, Belgium,
FINEP, CNPq, CAPES, FUJB and FAPERJ, Brazil,
Czech Ministry of Industry and Trade, GA CR 202/96/0450 and GA AVCR A1010521,
Danish Natural Research Council,
Commission of the European Communities (DG XII),
Direction des Sciences de la Matière, CEA, France,
Bundesministerium für Bildung, Wissenschaft, Forschung und Technologie, Germany,
General Secretariat for Research and Technology, Greece,
National Science Foundation (NWO) and Foundation for Research on Matter (FOM), The Netherlands,
Norwegian Research Council,
State Committee for Scientific Research, Poland, 2P03B06015, 2P03B1116 and SPUB/P03/178/98,
JNICT–Junta Nacional de Investigação Científica e Tecnológica, Portugal,
Vedecka grantova agentura MS SR, Slovakia, Nr. 95/5195/134,
Ministry of Science and Technology of the Republic of Slovenia,
CICYT, Spain, AEN96–1661 and AEN96-1681,
The Swedish Natural Science Research Council,
Particle Physics and Astronomy Research Council, UK,
Department of Energy, USA, DE–FG02–94ER40817.

References

[1] DELPHI Collaboration, P. Abreu et al., CERN-EP/98-180 (1998).
[2] ALEPH Collaboration, R. Barate et al., Phys. Lett. **B401** (1997) 150;
ALEPH Collaboration, D. Barate et al., Phys. Lett. **B401** (1997) 163;
L3 Collaboration, O. Adriani et al., Phys. Lett. **B307** (1993) 237;
OPAL Collaboration, K. Ackerstaff et al., Z. Phys. **C74** (1997) 1;
SLD Collaboration, SLAC-PUB-7481 (to be submitted to Phys. Rev. Lett.).
[3] DELPHI Collaboration, P. Abreu et al., Phys. Lett. **B405** (1997) 202;
ALEPH Collaboration, R. Barate et al., Phys. Lett. **B434** (1998) 437.
[4] D. J. Miller and M. H. Seymour, RAL-TR-98-042 (1998).
[5] V. Chabaud et al., Nucl. Inst. Meth. **A368** (1996) 314.
[6] DELPHI Collaboration, P. Abreu et al., Nucl. Inst. Meth. **A378** (1996) 57.
[7] N. Bingefors et al., Nucl. Inst. Meth. **A328** (1993) 447.
[8] S. Catani et al., Phys. Lett. **B269** (1991) 432;
N. Brown, W.J. Stirling, Z. Phys. **C53** (1992) 629.
[9] ALEPH Collaboration, D. Buskulic et al., Phys. Lett. **B313** (1993) 535.
[10] G. Borisov and C. Mariotti, Nucl. Inst. Meth. **A372** (1996) 181.
[11] T. Sjöstrand et al., in *"Z physics at LEP 1"*, CERN 89-08, CERN, Geneva, 1989;
Comp. Phys. Comm. **39** (1986) 347.
[12] T. Sjöstrand, Comp. Phys. Comm. **39** (1986) 347;
T. Sjöstrand and M. Bengtsson, Comp. Phys. Comm. **43** (1987) 367;
T. Sjöstrand, JETSET 7.3 manual, preprint CERN-TH6488/92(1992).
[13] The LEP Heavy Flavour Working Group, LEPHF 98-01.
[14] Particle Data Group, Eur. Phys. J. **C3** (1998).
[15] OPAL Collaboration, R. Akers et al., Phys. Lett. **B353** (1995) 59;
OPAL Collaboration, R. Akers et al., Z. Phys. **C67** (1995) 27.
[16] G. Marchesini et al., Comp. Phys. Comm. **67** (1992) 465.
[17] DELPHI Collaboration, P. Abreu et al., Z. Phys. **C73** (1996) 11.
[18] E. Accomando and A. Ballestrero, Comp. Phys. Comm. **99** (1997) 270.

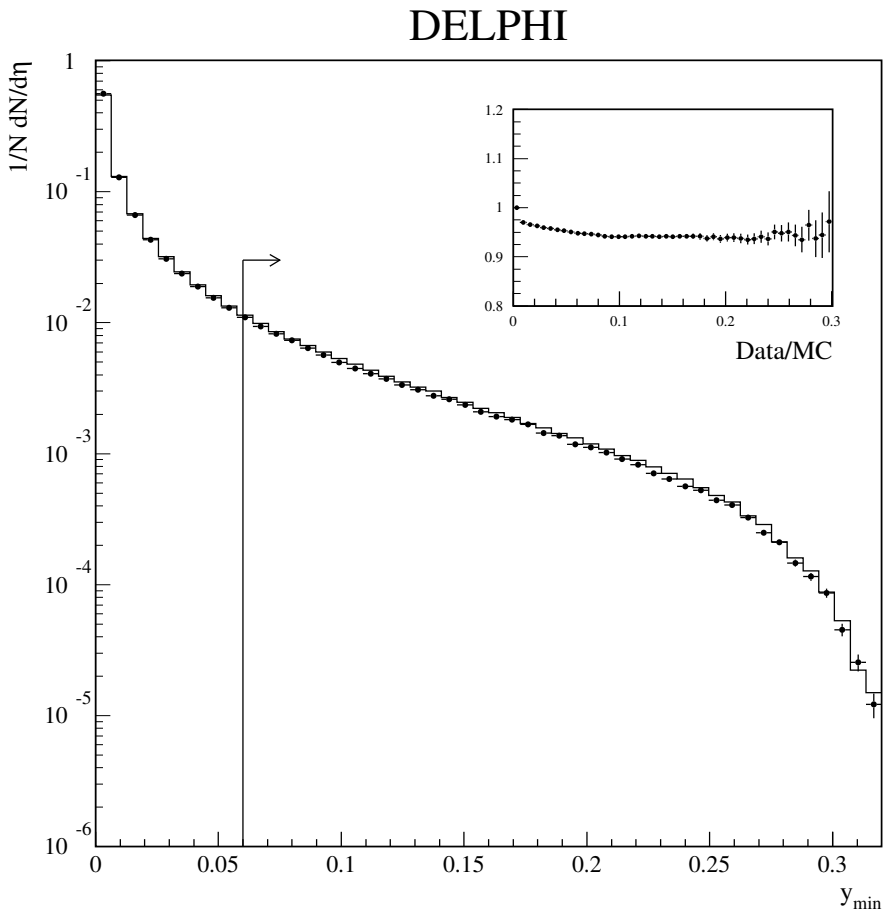

Figure 1: *Differential distribution of the y_{min} variable for real data (dots) and simulation (histogram). The ratio of the cumulative distributions is shown in the inset. The value of the cut is indicated by the arrow.*

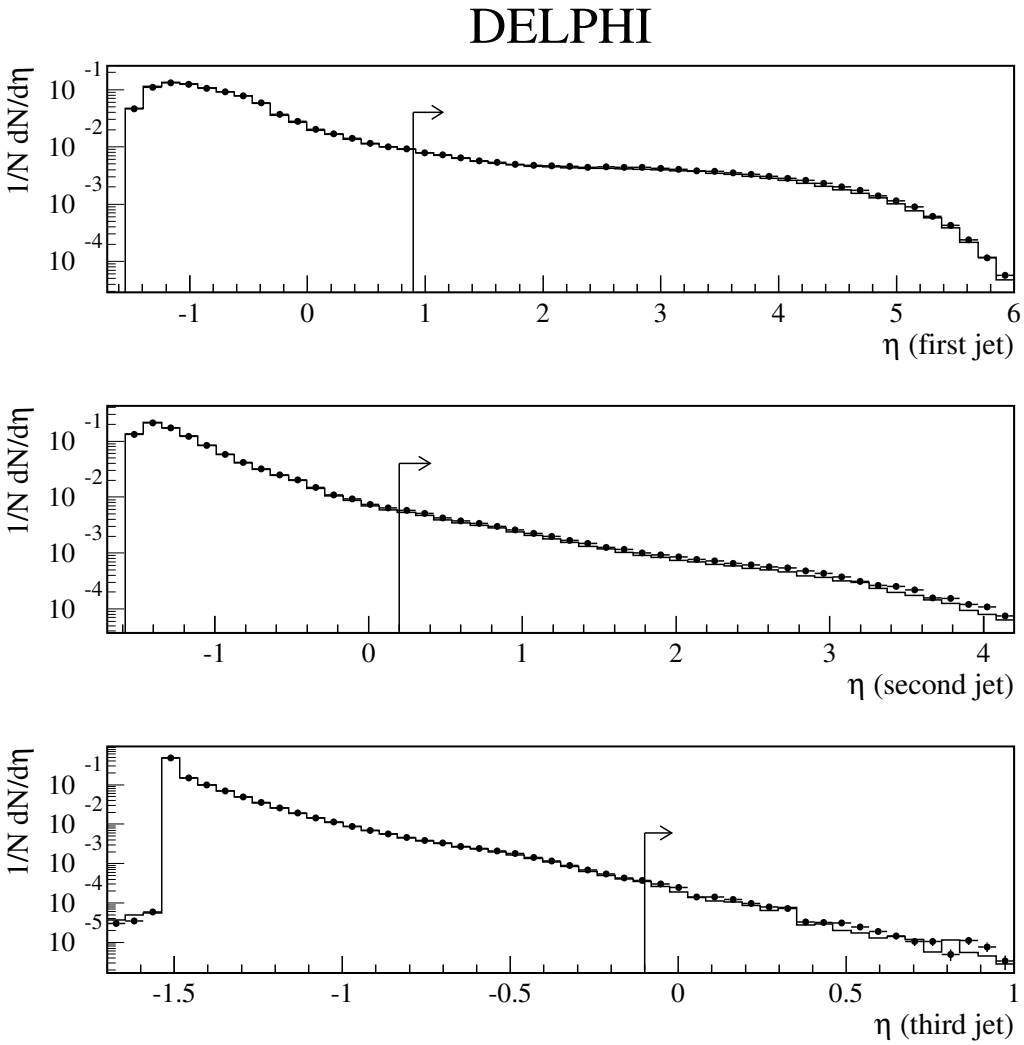

Figure 2: *Differential distribution of the b-tagging variables for the three ordered jets for data (dots) and simulation (histogram). The drop at $\eta = 1.5$ for the third jet is related to the different definitions of the b-tagging variable for jets with and without a reconstructed secondary vertex. The values of the cuts are indicated by the arrows.*

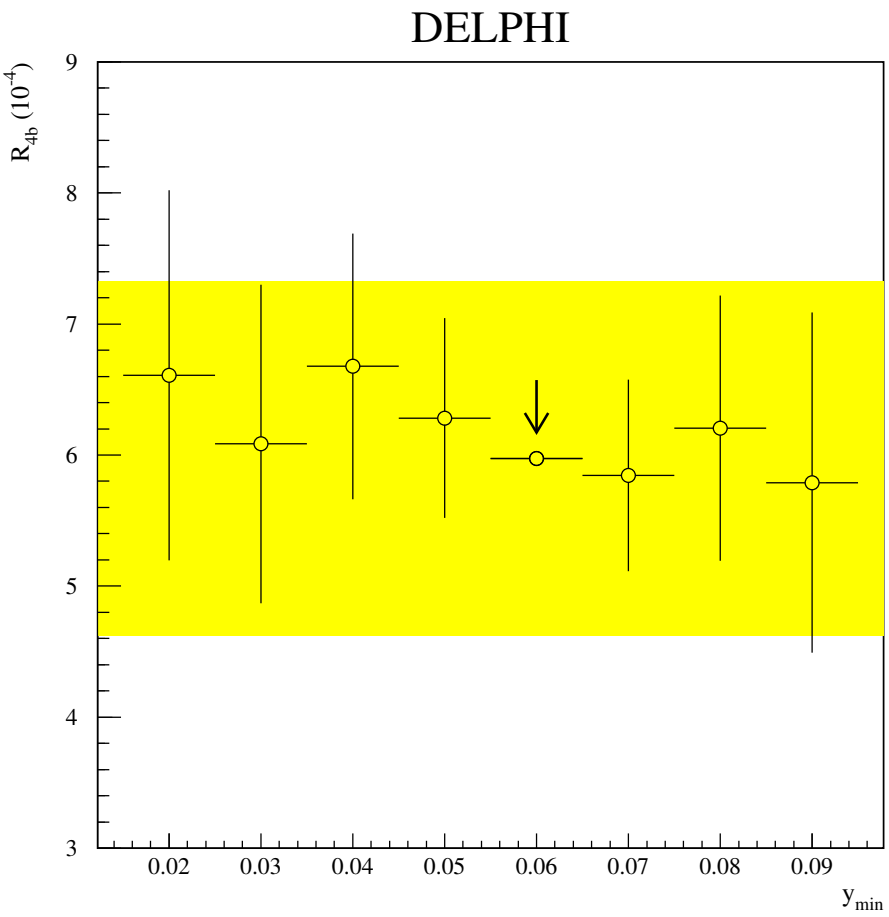

Figure 3: *Stability of the result as a function of the y_{min} cut. The bars represent the uncorrelated statistical errors referred to the central cut at 0.06. The shaded band represents the systematic error.*

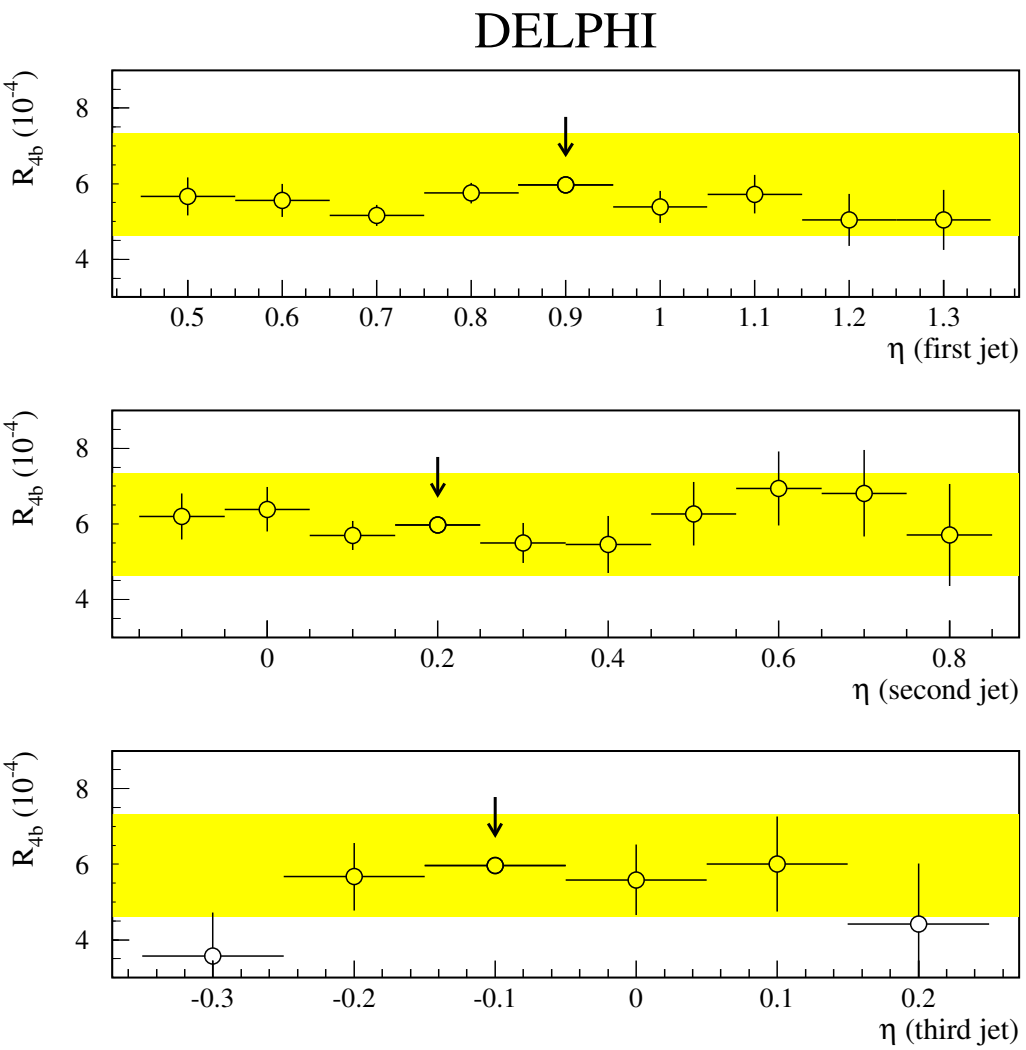

Figure 4: *Stability of the result as a function of the b-tagging variables for the three ordered jets. The bars represent the uncorrelated statistical errors referred to the central cuts at 0.9, 0.2, -0.1 respectively. The shaded bands represent the systematic error.*

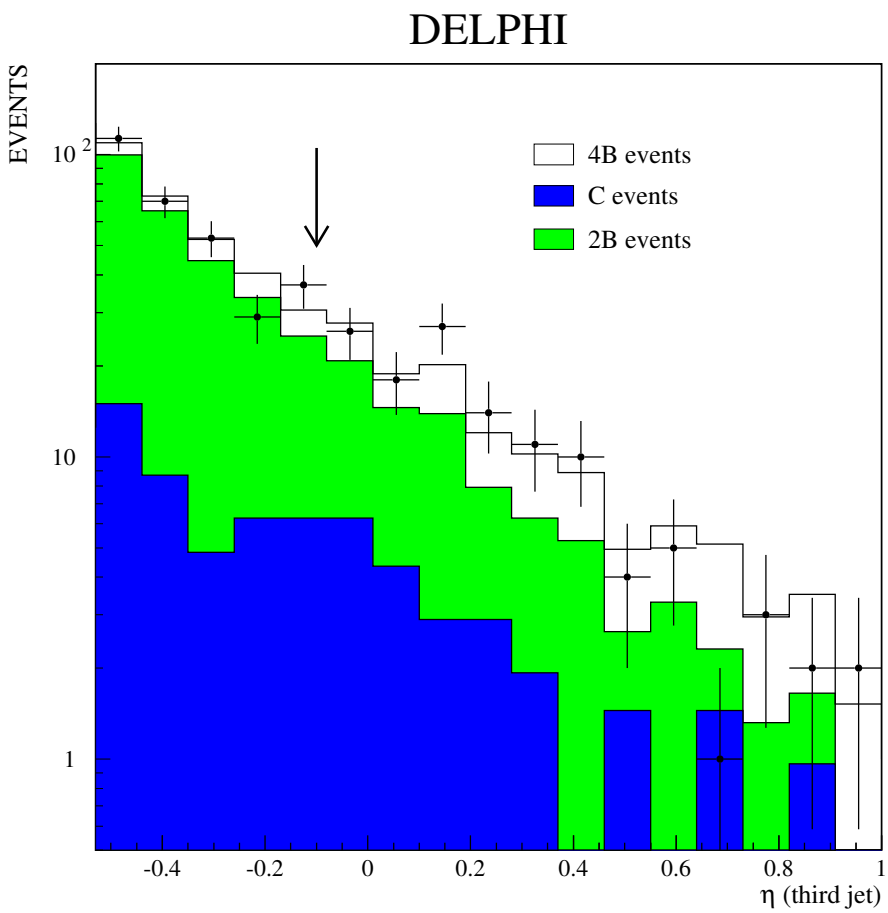

Figure 5: *Distribution of the b-tagging variable η for the third jet for data (dots) and simulation (histograms) after all other cuts.*

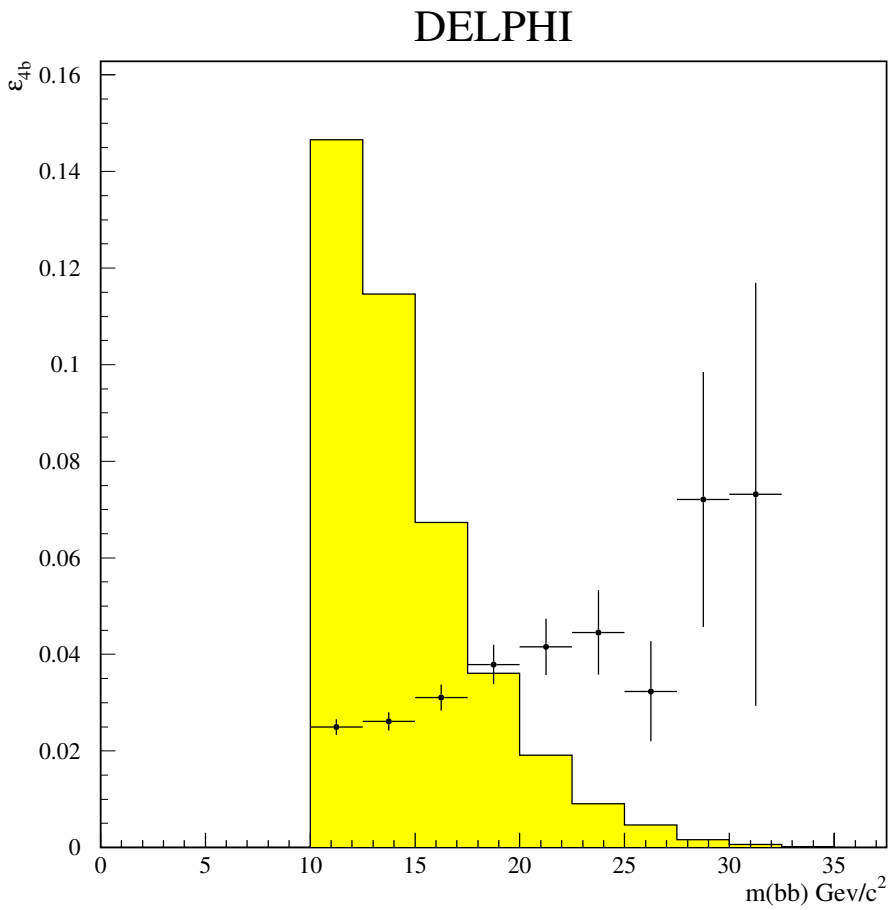

Figure 6: *The signal efficiency ϵ_{4b} as a function of the minimum invariant mass between b quark pairs. The histogram represents the generated spectrum in JETSET PS simulation (arbitrary units).*